ISBN: 978-3-95450-214-1 ISSN: 2673-5490 doi:10.18429/JACoW-IPAC2021-WEPAB123

MULTI-BUNCH RESISTIVE WALL WAKE FIELD TRACKING VIA PSEUDOMODES IN THE ALS-U ACCUMULATOR RING

M. P. Ehrlichman*, S. De Santis, T. Hellert, S. C. Leemann, G. Penn, C. Steier, C. Sun, M. Venturini, D. Wang, Lawrence Berkeley National Laboratory, Berkeley, USA

Abstract

For the ALS-U project, particles will be injected from the booster to the accumulator ring utilizing an injection scheme that leaves the stored and injected particles with a non-trivial transient. This transient requires that multibunch feedback be masked for those buckets into which charge is injected. The masking significantly diminishes the damping capability of the multibunch feedback system. This problem is exacerbated by the large injection transient. The higher order multibunch resistive wall wake fields in the accumulator ring exceed the radiation damping time. To study whether the beam will remain multibunch stable during the injection transient, a multibunch tracking simulation is used that simulates the multibunch feedback system and also pseudo-mode representation of resistive wall wake fields.

INTRODUCTION

The ALS-U accumulator ring (AR) will be situated between the full energy booster and storage ring to facilitate swap-out injection of an entire bunch train. Depleted trains from the storage ring will be swapped one at a time with replenished trains from the accumulator ring.

Injection into the AR from the booster will be facilitated using a three-dipole kicker off-axis injection scheme [1]. Injected charge, in the shape of 4 consecutive shots spaced 3 buckets apart, will arrive via a pulsed thin septum. The injected charge will be placed on a stable trajectory by a single-turn ferrite-loaded kicker, which will at the same time also kick the stored beam. The stored beam will have been pre-kicked by two dipole kickers situated in the two preceding arcs. The pre-kicks place the stored beam on a trajectory that partly compensates for the kick received from the main injection kicker.

Figure 1 shows the trajectories of the stored and injected particles following an injection cycle. The centroid of the injected particles has an RMS amplitude of 0.734 mm, while that of the stored beam is larger, 2.44 mm. Note that the stored beam has an emittance of 1.8 nm-rad and the injected beam is much larger with an emittance of 300 nm-rad.

The bunch-by-bunch feedback system (TFB) will detect the transient of the stored beam and apply kicks to damp it. Unfortunately, those kicks will anti-damp the injected particles since the stored beam and injected particles are 180° out of phase. The injected particles carry relatively little charge and will offset only slightly the center-of-charge that the feedback system detects. To prevent the loss of injected particles as the TFB damps the injection transient, the TFB will be masked for those buckets into which charge is injected. A single injection shot delivers charge into 4 buckets, spaced 3 buckets apart, for example, buckets 10, 14, 18, and 22.

While the AR beam is multibunch stable vs HOM modes with radiation damping alone, the highest order resistive wall (RW) modes exceed the radiation damping rate and multibunch feedback will be necessary to maintain stability. Masking the 4 buckets from the TFB will significantly reduce the damping rate the TFB can apply to the beam. To determine whether the beam in the AR will remain multibunch stable vs resistive wall effects we undertook a multi-bunch tracking simulation that includes resistive wall wake fields documented here. This study follows closely that presented in [2]. This simulation was developed using the *Bmad* subroutine library [3].

* mike@lbl.gov

PSEUDO-MODES REPRESENTATION OF RESISTIVE WALL WAKES

The long-range resistive wall wake is,

$$W(t) = \frac{\sqrt{c}}{\pi b^3}\sqrt{\frac{Z_0}{\pi\sigma}}\frac{L}{\sqrt{t}}, \tag{1}$$

where b is the chamber dimension and σ its conductivity [4]. c and Z_0 are the speed of light and impedance of free space, respectively. L is the length of the chamber and t is time since the passage of the generating particle. This equation is valid when

$$-z \gg \sqrt[3]{\frac{b^2}{Z_0\sigma}}. \tag{2}$$

Among the various accumulator ring chamber types, the right hand side of Eq. (2) is at most 0.1 mm. This is much less than the bunch spacing of 0.6 m.

To the $t^{-1/2}$ dependence of Eq. (1) we fit a basis of pseudo-modes,

$$W_i(t) = \frac{A_i^2}{S_i^2}\exp\left(-\frac{d_i^2}{S_i^2}t\right), \tag{3}$$

where A_i, S_i, and d_i are fit parameters. S_i is redundant but has been found to ease numerical fitting. Fifteen terms are used in the basis and `Mathematica`'s `NonlinearModelFit` is used for the fitting, which reliably converges after a few moments. The residuals of the fit are less than 0.1% from 1 ns to 26.7 ms, and reliably decay to zero beyond the ends of the fit, as shown in Fig. 2. The same fit is used for all chambers, but is scaled according to the local chamber properties using the coefficients in Eq. (1).

TRACKING SIMULATION

The tracking simulation is developed in `Bmad`. Twenty-six bunches are tracked, with each bunch represented by a

ISBN: 978-3-95450-214-1 ISSN: 2673-5490 doi:10.18429/JACoW-IPAC2021-WEPAB123

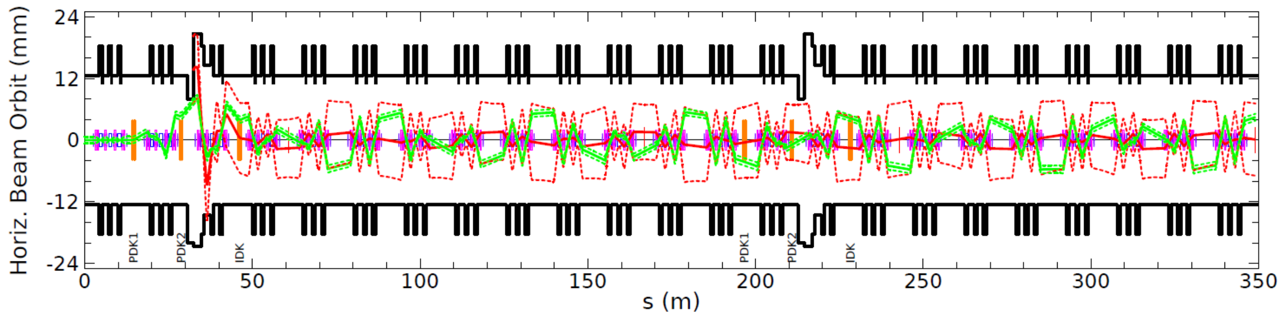

Figure 1: Trajectories of stored (green) and injected (red) particles following an injection cycle. Solid lines represent centroid, dashed lines represent 3-σ of the beam dimensions. The two pre-kickers and main injection kicker are labeled PDK1, PDK2, and IDK.

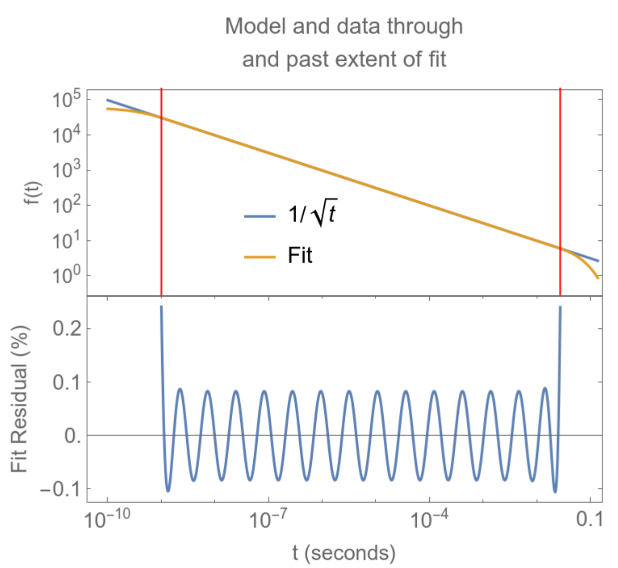

Figure 2: Fit of pseudomodes to the $1/\sqrt{t}$ dependence of the long-range resistive wall wake. The vertical red bars indicate the fitted region, which extends from 1 ns to 26.7 ms (equivalently said: one-half of a 500 MHz bucket to 44000 turns). Within the fitted region, the fit is good to 0.1%. Outside the region, the fit reliably decays to zero.

single fully charged, 1.1 nC marco particle. The resistive wall wakes are represented at 216 locations in the ring by the pseudo-mode fit, scaled by the appriorate coefficients for the local chamber material and dimensions. Bmad automatically keeps track of the RW pseudo-modes as they build up over the duration of the simulation. Radiation damping is implemented by applying a per-turn damping decrement to the action of each macro-particle.

The ALS-U AR will include multi-bunch damping in all 3 planes provided by Dimtel iGp feedback controllers [5]. These are represented in simulation using a pickup, kicker, and FIR filter that replicates the iGp FIR filter. The power of the simulated feedback system is controlled by setting a saturation level for the max kick. The saturation is obtained from models of the actual stripline kicker design and is 1.1 µrad.

The simulation is run independently for each transverse plane for each of the 26 multi-bunch modes. For each mode j, each bunch i of the train is seeded with an initial offset,

$$x_i = \sqrt{J_x \beta_x} \cos\left(\frac{\pi}{2} + \frac{2\pi i j}{N_{bunches}}\right) \tag{4}$$

$$x_i' = \sqrt{\frac{J_x}{\beta_x}} \left(\alpha_x \cos\left(\frac{\pi}{2} + \frac{2\pi i j}{N_{bunches}}\right) + \sin\left(\frac{\pi}{2} + \frac{2\pi i j}{N_{bunches}}\right)\right), \tag{5}$$

where J_x is the action (arbitrarily set to a small amplitude of 2 nm), β_x and α_x are Twiss functions, and $N_{bunches}$ is the number of bunches in the train. A similar equation is applied when simulating vertical modes.

The train is tracked for 5000 turns. Each turn the normal mode coordinates of each bunch are recorded and a Fourier transform of the action is taken along the bunch train. For the seeded mode, the growth rate is obtained from the fit of an exponential to the the height of the spectral peak versus turn number.

PER-MODE RESULTS

The growth rates of each of the 26 modes obtained from the simulation are shown in Fig. 3. Each data point represents a separate 5000 turn tracking simulation. The “no damping, no TFB” case shows the resistive wall growth rates in the absence of radiation damping and with no multibunch feedback. The “w/ Rad. Only” case demonstrates that all horizontal modes are stable with radiation damping alone, though the highest order vertical modes remain unstable. The “w/ Rad. Damping, unmasked TFB” represents steady-state conditions, long after an injection cycle, with radiation damping and unmasked TFB. The modes in this case are all very well damped. The “w/ Rad. Damping, masked TFB” shows the growth rates of each mode during the injection transient when the TFB is masked for those 4 buckets into which charge has been injected.

From Fig. 3 we conclude that while masking will significantly reduce the damping obtained from the multibunch feedback system, all resistive wall modes will remain stable by a comfortable margin during the injection transient.

ISBN: 978-3-95450-214-1 ISSN: 2673-5490 doi:10.18429/JACoW-IPAC2021-WEPAB123

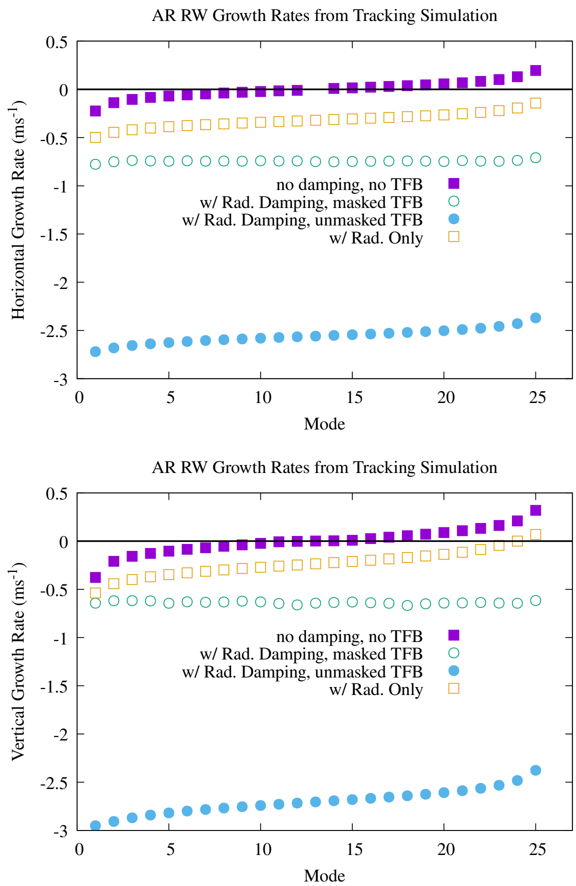

Figure 3: Per-mode growth rates of a 26 bunch train in the accumulator ring determined by multi-bunch tracking with resistive wall wake fields. During steady-state, all RW modes are safely damped with a total growth rate of about $-2.5\,\mathrm{ms}^{-1}$. The radiation damping rate is $0.16\,\mathrm{ms}^{-1}$. During the injection transient the effectiveness of the TFB is significantly diminished by the necessity of masking the 4 buckets into which charge is injected from the feedback pattern, though all modes remain damped.

LARGE AMPLITUDE SIMULATION

The simulation described in the preceding section evaluates the growth rates of the individual RW modes in the presence of multibunch feedback and radiation damping. Obtaining a reliable measurement of the growth rates from the simulation requires small oscillation amplitudes. However, following an injection cycle, the beam is left with a large transient that samples non-linearities in the lattice. To evaluate absolute stability following an injection cycle, the beam is given a uniform 5 mm horizontal offset and tracked for 5000 turns. Without masking, after 1702 turns the bunch oscillating with the largest amplitude has an action that is 50% of the initial condition. With 4 bunches masked, 50% is achieved after 3266 turns. All pseudomodes are reliably decaying in strength throughout the simulation.

Figure 4 shows the maximum kick applied by the horizontal TFB following the injection cycle. The TFB remains in saturation for roughly 4400 turns.

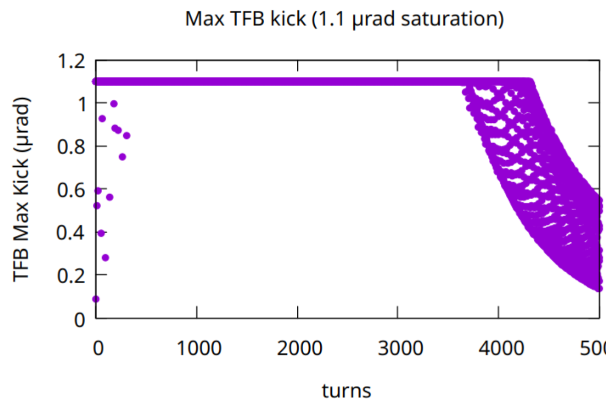

Figure 4: Per-turn maximum kick applied by the horizontal TFB following an injection transient, with 4 buckets masked. The saturation limit of 1.1 µm is set by the stripline kicker geometry and the multibunch feedback amplifier. The feedback system comes out of saturation after approximately 4400 turns.

CONCLUSION

The ALS-U AR will implement a novel three-dipole kicker injection scheme that leaves the stored and injected particles with a non-negligible injection transient. One consequence of this transient is that the multibunch feedback system will need to be masked for certain buckets. In this study, we have demonstrated that the beam will remain multibunch stable by a comfortable margin versus resistive wall instabilities during the injection transient.

REFERENCES

[1] M. P. Ehrlichman *et al.*, "The Three Dipole Kicker Injection Scheme for the ALS-U Accumulator Ring", presented at the 12th Int. Particle Accelerator Conf. (IPAC'21), Campinas, Brazil, May 2021, paper WEPAB124.

[2] S. Wang, M. G. Billing, S. Poprocki, D. L. Rubin, and D. Sagan, "Resistive Wall Instability and Impedance Studies of Narrow Undulator Chamber in CHESS-U", in *Proc. 8th Int. Particle Accelerator Conf. (IPAC'17)*, Copenhagen, Denmark, May 2017, pp. 3204–3207. doi:10.18429/JACoW-IPAC2017-WEPIK110

[3] D. Sagan, "Bmad: A relativistic charged particle simulation library", *Nucl. Instrum. Methods Phys. Res., Sect. A*, vol. 558, no. 1, pp. 356–359, Mar. 2006. https://doi.org/10.1016/j.nima.2005.11.001

[4] A. W. Chao, *Physics of Collective Beam Instabilities in High Energy Accelerators*, New Jersey, United States: John Wiley & Sons, 1993.

[5] *iGp12-328F Signal Processor - Technical User Manual*, D. Teytelman, Dimtel Inc., CA, USA, Jul. 3, 2019, pp 1–93. https://www.dimtel.com/_media/support/manuals/manual12_328f_screen.pdf